Revista Mexicana de Ciencias Agrícolas

DOI: https://doi.org/10.29312/remexca.v16i1.3369

Article

Estimation of agricultural areas through cloud processing for the Potosino highlands

José de Jesús Hernández-Ramos[1]
José Pimentel-López[1,§]
Alejandro Amante-Orozco[1]
Esteban Salvador Osuna-Ceja[2]

1 Maestría en Ciencias en Innovación en Manejo de Recursos Naturales-Campus San Luis Potosí-Colegio de Postgraduados. Iturbide 73, Salinas de Hidalgo, San Luis Potosí, México. CP. 78600.

2 Campo Experimental Pabellón-INIFAP. Carretera Aguascalientes-Zacatecas km 32.5, Pabellón de Arteaga, Aguascalientes, México. CP. 20660.

Autor para correspondencia: josep@colpos.mx

Abstract

Optical satellite imagery is a powerful information bank for estimating agricultural areas. This study aimed to estimate agricultural areas in the municipalities of Salinas, Santo Domingo, and Villa de Ramos through cloud processing of satellite images and their comparison with the traditional-INEGI technology. The work was carried out limited to the agricultural area, which totals an area of 190 871 ha, of which 86% are rainfed. The study period was from October 2020 to October 2021. Six classification algorithms were applied; three for traditional-INEGI: minimum distance, maximum likelihood, and spectral angle mapper in QGIS 3.18; and three for cloud processing: classification and regression trees, random forest, and support vector machine with Google Earth Engine. The areas of the main crops (corn, beans, oats, alfalfa, and chili) were estimated for the study area based on 294 field samples. For Sentinel-2 image processing, a cloud-free geomedian was used. The results of the confusion matrices indicated which classifications were more accurate; the values were 89% for classification and regression trees and random forest, 59% for support vector machine, 48% for minimum distance, 43% for maximum likelihood, and 46% for spectral angle mapper. The classification and regression trees and random forest algorithms outperformed the other classifiers evaluated in accuracy, estimating the corn and bean agricultural areas closest to each other (80 131 and 98 138 ha in corn and 60 174 and 60 358 ha in beans) compared to the remaining classifiers.

Keywords:

crops, google earth engine, QGIS.

DOI: https://doi.org/10.29312/remexca.v16i1.3369

Introduction

SIAP (2020) reports that the municipalities of Salinas, Villa de Ramos and Santo Domingo cover an agricultural area of 190 871 ha, of which 86% are rainfed. Under this condition, the main crops planted are corn and beans. Given their importance in the region, it is necessary to have continuous and spatially distributed agricultural information during the production cycle of these crops. Therefore, it is convenient to use remote sensing techniques that have been more accepted for the processing of remote sensing data due to the advances that this discipline has had (Romero, 2016; Gallardo-Cruz *et al*., 2019).

The combination of remote sensing with agronomy gives rise to a specific research topic, where specialists have a field of analysis for a very varied field of application, especially in recent years with the application of infrastructures for the processing of large volumes of data in the cloud (Aguilar, 2016). The National Institute of Statistics and Geography (INEGI, for its acronym in Spanish) applies a methodology for the estimation of agricultural areas that requires considerable human, economic, and computer resources.

Nevertheless, cloud computing combined with remote sensing techniques can offer better optimization of human and computer resources. The combination of cloud processing disciplines with others has been reported, where specialists in land use and vegetation participate (Killough, 2018; Vega *et al*., 2019; Venkatappa *et al*., 2019; Aghababaei *et al*., 2021).

It was known that there are few studies registered in the specialized literature that address cloud processing and agricultural areas, such as those by German *et al*. (2019); Mananze *et al*. (2020); Amani *et al*. (2020). German *et al*. (2019) applied support vector machine and random forest algorithms to estimate vegetable areas in the periphery of La Plata, Argentina, and obtained an accuracy between 96% and 98%.

The algorithms proposed here can yield good results in cloud computing despite the fact that, in this case, the structure of the plantations of the crops of interest are totally different, since they are mostly concentrated in rainfed areas and for this reason, crops such as beans have a low vegetation cover, which also occurs for oat and corn crops in early stages, so the exposure of bare soil predominates and is what is finally captured by the satellite image.

Regarding processing in computer equipment, there are studies such as that by TA *et al*. (2022), who worked with ecological environments in Sinaloa, Mexico, where they applied the maximum likelihood algorithm and managed to obtain up to 87% accuracy. Based on this background, the present work was carried out with the aim of estimating the agricultural areas of three municipalities of the northwest Potosino highlands through cloud processing of satellite images and their comparison with the traditional-INEGI technology, and evaluating the results of the six algorithms used.

Materials and methods

The municipalities studied are located in the northwest Potosino highlands on the border with the state of Zacatecas (Figure 1). The predominant climate in the region is dry temperate and semidry temperate according to INEGI (2008). Annual rainfall ranges between 300 and 400 mm and there is a regime of rains in summer and winter precipitation less than 5% of the annual record (CONAGUA, 2020). The average annual temperature varies between 12 and 18 °C. The municipal area, which includes the areas of Salinas, Villa de Ramos, and Santo Domingo, reaches 845 250 ha, of which 190 871 ha are agricultural (SIAP, 2020); most of this area is located in the municipality of Villa de Ramos with 104 760 ha.

Revista Mexicana de Ciencias Agrícolas

DOI: https://doi.org/10.29312/remexca.v16i1.3369

Figure 1. Location of the study area.

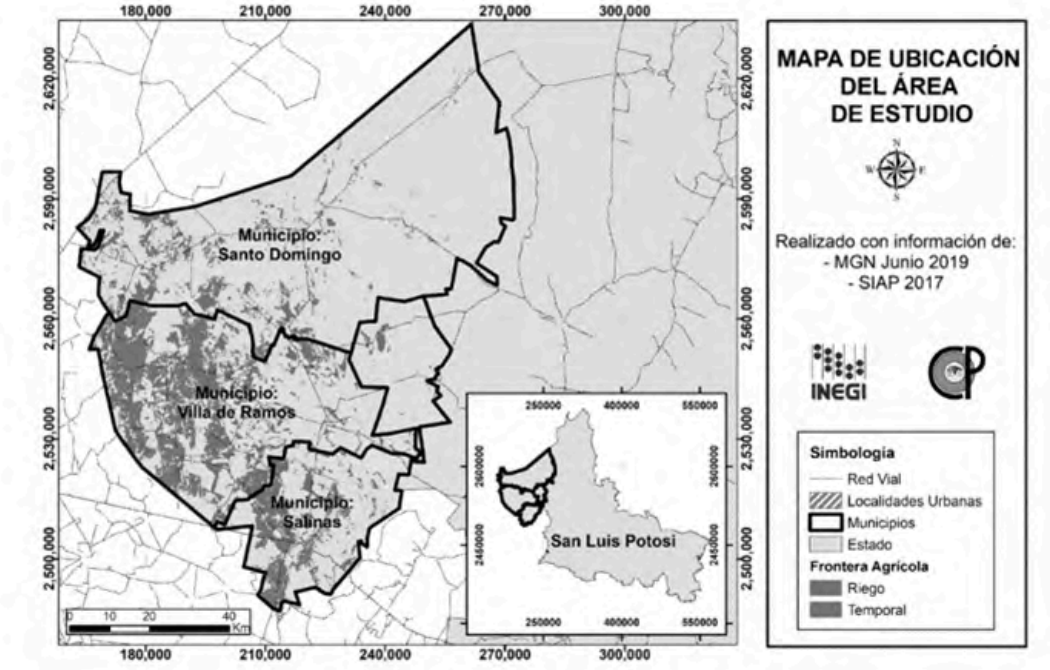

The information was obtained from October 2020 to October 2021 and was used to estimate the agricultural area in the 2020 spring-summer (SS) cycle in the three municipalities studied. This research evaluated the different algorithms that exist in the literature to perform feature extraction on regions of interest in a satellite image and different intelligent algorithms to carry out the classification based on patterns in order to propose an improvement in the methodology that allows efficient crop classification.

This work was divided into five stages: the first consisted of acquiring satellite images from the Sentinel-2 MSI multi spectral instrument, level-2A, in the Copernicus platform. The spatial resolution used was 10 (B2, B3, B4 and B8) and 20 (B5, B6, B7, B8A, B11 and B12) meters at the same time. The field sampling was carried out from October 19 to 23, 2020; the second focused on applying the algorithms for extracting the spectral signatures; the third consisted of cutting out the image of each municipality; the fourth was aimed at the training of the different intelligent algorithms that will allow classifying the descriptive features obtained in the first stage; and the last consisted of the validation of the performance of the classifier by using 43 samples other than those used in training (Figure 2).

Revista Mexicana de Ciencias Agrícolas
DOI: https://doi.org/10.29312/remexca.v16i1.3369

Figure 2. Methodology flowchart.

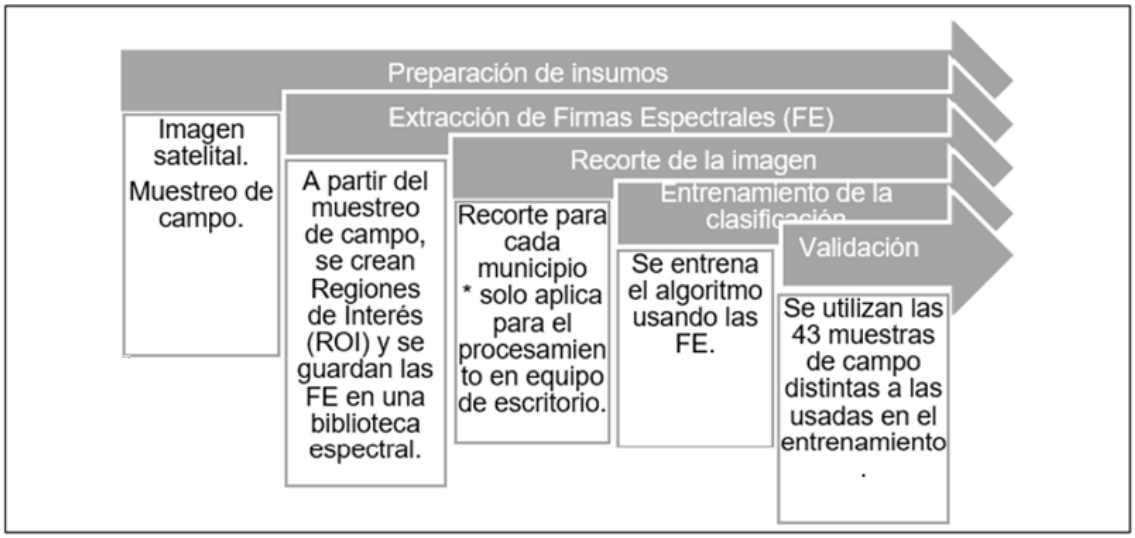

The field information that was collected in the studied territory had as a reference the universe of 34 132 plots of land that include ejido property and small property, for the three municipalities (INEGI, 2020a). For field sampling, it was planned to characterize 380 plots of these sites, which were randomly selected using the random selection tool of QGIS v.2.18.

On the other hand, field data was collected in a QField v.3.3.0 project, which was divided into four sections: location of the sample, detail of the crop, photos, and general description. The location included the national geostatistical framework (NGF) and the geostatistical names and keys where each plot was located, which are data that cannot be edited on the mobile device.

In the detail of the crop, only the type, its phenological stage, and any damage if it existed were defined. In the photo section, a couple of images were captured with the camera of the mobile device: a panoramic photo and photo of the plants, which were linked to each plot. The field samples were used to define the regions of interest (ROI) and train the supervised classifications. First, we worked on the Google Earth Engine (GEE) platform with the support of the intake of vector files for the digitization of ROIs; in this, we used random forest (RF) algorithms that work with individual decision trees, which creates a slightly different data for each tree (Panagiotakis *et al*., 2021).

The second algorithm was classification and regression trees (CART), which works through decision trees for regression and classification of data (Strzelecka and Zawadzka, 2021) and finally, the third algorithm used in GEE was support vector machine (SVM), which works by correlating data in a large space in such a way that training regions can be categorized (Sánchez-Pozo *et al*., 2021; Kok *et al*., 2021).

The same image was classified on a computer with the following characteristics: Intel® Core™ i7 processor, 32 GB RAM, 64-bit Windows operating system, where the following algorithms were used: minimum distance (MD), maximum likelihood (ML), and spectral angle mapper (SAM) in the QGIS 3.18 software and the semi-automatic classification plugin (SCP). To execute the process, the spectral signatures (SS) of each ROI were extracted, these were stored in a spectral library and then the FEs were applied to the satellite imagery for each algorithm.

To validate the results, 43 field samples that were collected on the same date and study area were used. These samples were used to create 43 ROIs, which were entered into the project and the confusion matrix algorithm of each classified image was run versus the 43 ROIs. Subsequently, in the monitoring of rainfall, the monthly climate products offered by TerraClimate of the land surface were used. TerraClimate uses climate-assisted interpolation, which combines normalized climatological data from the WorldClim dataset (Abatzoglou et al., 2018).

DOI: https://doi.org/10.29312/remexca.v16i1.3369

The estimation of the geomedian used a series of images obtained mainly from the 14QKL mesh since it covers most of the area of interest; the following images were also employed: 14QKM, 13QHF, 13QHG, 13QGF, and 13QGG. Geomedian is defined as a high-dimensional statistic that exchanges a time series of Earth observation images for a single high-quality composite pixel with reduced spatial noise that maintains its spatial consistency (Roberts *et al*., 2017).

The geomedian is particularly useful when the probability distribution of the data is not necessarily multivariate normal or if there are outliers in the data (Roberts *et al*., 2017; INEGI, 2020b). Finally, the Normalized Difference Vegetation Index (NDVI) was calculated at 5-day intervals during the SS cycle for the sampled ROIs. The information obtained was employed to analyze the average behavior and sustained trend of the NDVI in the rainfed and irrigated agricultural areas of the three municipalities under study; from the behavior of the index, the date of greatest vigor of the crops was identified.

Results and discussion

The behavior of NDVI identified the highest peak in vegetation development in September 2020; this month was taken as the optimal date to detect all crops at their highest vigor. The analysis of results showed that, in the study area, the precipitation pattern is characterized by a strong interseasonal and interannual variability, which in turn governs the start of sowing of rainfed crops for the spring-summer cycle.

The seasonal magnitude of precipitation in the northwest Potosino highlands is recorded on average as follows: summer, autumn, winter and spring with 53.2%, 20.4%, 14.3% and 12.1% of the total annual precipitation, respectively. It was considered that the large variation in total annual precipitation originates in the fluctuation of the number of precipitation events rather than in their magnitude and is responsible for the occurrence and length of the intra-summer drought or heat wave, which is known to occur in these semi-arid areas (Bravo *et al*., 2006; Núñez-López *et al*., 2007).

On the other hand, the sampling results were not as expected according to plan; 294 samples were obtained out of the 380 indicated in the sample size; the reason for not meeting the sampling objective was the time available for sampling due to the early harvests in the area. Of the samples collected: 102 were beans, 101 corn, 7 alfalfa, 5 oats, 6 chili, 35 other crops (which mainly included the combination of two or more crops in the same plot), and finally, 38 samples without crops.

The estimated distribution of the different crops using the CART algorithm, processed in GEE, is shown in Figure 3. It can be noted that the dominant crops in the sown area are corn and beans; in these cases, the crops of the same type, both irrigated and rainfed, were grouped. Nonetheless, according to what was observed during the sampling, oat, alfalfa, and chili crops are spatially distributed in the irrigated areas.

DOI: https://doi.org/10.29312/remexca.v16i1.3369

Figure 3 . Spatial distribution of the crops estimated using the CART algorithm.

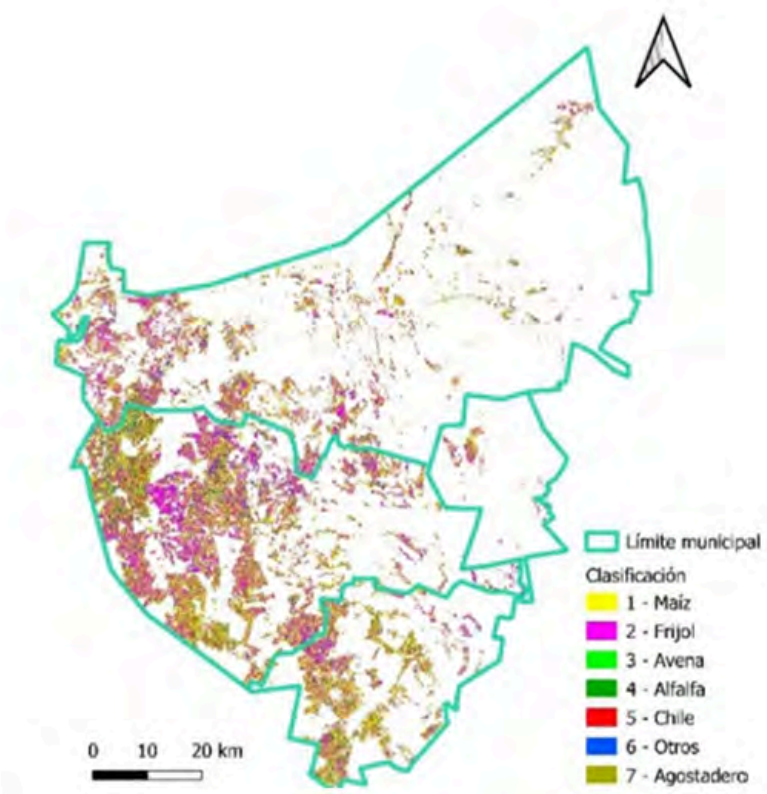

Two hundred ninety-four ROIs were digitized and used to train the classifications in each algorithm. These were homogeneous polygons of the same spectral range to reduce the confusion that could occur between the classes. Table 1 presents the results of the estimated area for each of the crops evaluated with the six algorithms employed. In general, it was observed that the areas estimated with the three algorithms (CART, RF, and SVM) applied in GEE were higher than those estimated with the three algorithms (ML, MD, and SAM) in QGIS for all cases.

Table 1. Estimated areas in hectares for the different algorithms by crop.

Crop	SVM	CART	RF	ML	SAM	MD	SIAP
Corn	110 706	80 131	98 138	55 472	75 621	78 265	41 435
Beans	52 565	60 174	60 358	77 794	46 686	48 553	89 605
Oats	2 988	1 921	1 538	1 914	1 724	3 341	6 850
Alfalfa	5 402	5 019	3 503	1 514	4 434	2 625	2 780
Chili	2 741	5 642	3 979	735	2 272	3 111	16 552
Others	1 914	23 442	14 211	12 149	15 154	12 968	1 029
Without crops	25 867	25 853	20 454	16 436	17 469	15 420	-
Total	202 182	202 182	202 182	166 015	163 359	164 282	158 251

MD= minimum distance; ML= maximum likelihood; SAM= spectral angle mapper; CART= classification and regression trees; RF= random forest; SVM= support vector machine.

DOI: https://doi.org/10.29312/remexca.v16i1.3369

According to these results, the largest area estimated with all the classifiers was that for corn, then beans and finally, irrigated crops (alfalfa, chili, and oats); in addition, others and without crops were also included. Thus, corn and bean crops are the most common and the most important in the study area since they add up to an estimated average area of 140 744 ha for the studied cycle. Regarding the area reported by SIAP (2021) for the cycle studied, the estimated area differs greatly with most of the algorithms applied for all the crops evaluated.

The discrepancies observed, especially in irrigated crops, are probably due to the spatial distribution of the samples that were used to train the algorithms. The estimated processing times for each algorithm are shown in Table 2. In the case of training, it included the creation, modification and debugging of the ROIs, which served to train the other algorithms within the same platform.

Table 2. Average processing times (in hours).

	Training	Classification execution	Image download	Confusion matrix calculation	Total
GEE	5.25*	0.25	0.25	0.25	6
QGIS	6*	15	0	5	26

* = It includes the creation of the ROIs for a single occasion since they will be the same training polygons for all the algorithms.

The cloud processing time used in the 294 ROIs was 6 h per algorithm, whereas the time required for the execution of each algorithm with the same ROIs, applied in desktop software (QGIS 3.18), was up to 26 hours. This 20-hour difference is due to the GEE engines that function as servers for processing. This time saving coincides with what was reported by Perilla and Mas (2020) in the sense that GEE is a powerful tool that links the potential of big data and the efficiency of cloud processing.

Therefore, processing times were significantly faster in the cloud than on desktop, which ensures savings in economic, computer, and human resources. The validation of the results was determined by the confusion matrix of each algorithm; this matrix was obtained by comparing the predicted data *versus* the observed data, which corresponded to the 43 samples that were not used in the training. This identifies how many pixels were correctly classified and how many were confused with another crop, which was done for each of the 7 classes.

The classes obtained were defined as follows: 1 for corn, 2 for beans, 3 for oats, 4 for alfalfa, 5 for chili, 6 for other crops that are combined, and finally, class 7 for plots without crops or at rest. For the calculation of error matrices that represent the probability that sampled areas in the image are correctly classified with the sum of those pixels that were correctly classified. This meant that the predicted value and the observed value correspond to the same class, so there is a number of pixels correctly classified.

The quotient of this value was calculated; it was divided by the total number of pixels and a percentage of accuracy for each classification was obtained. In the case of the SVM algorithm, there was a slight confusion between class 2 of the predicted values and class 1 of the observed values and between classes 6 and 1 (28 pixels); in this case, an accuracy of 59% was obtained (Table 3).

Table 3. Confusion matrix for the SVM algorithm.

SVM		Predicted values							Total
		1	2	3	4	5	6	7	
Observed values	1	95	68	0	0	0	28	11	202
	2	15	89	0	0	0	0	3	107
	3	0	0	0	0	0	0	0	0

DOI: https://doi.org/10.29312/remexca.v16i1.3369

SVM	Predicted values							Total
	1	2	3	4	5	6	7	
4	0	0	0	0	0	0	0	0
5	0	0	0	0	0	0	0	0
6	0	0	0	0	0	0	0	0
7	5	0	0	0	0	1	1	7
Total	115	157	0	0	0	29	15	185
			TP+TN					185
			TP+FP+FN+TN					316
			Accuracy					59%

TP= true positive; TN= true negative; FP= false positive; FN= false negative.

In the case of the CART algorithm, low confusion was detected and it was mainly between classes 1 and 2. This algorithm yielded an accuracy of 89% in 281 pixels out of 316 (Table 4).

Table 4. Confusion matrix for the CART algorithm.

CART		Predicted values							Total
		1	2	3	4	5	6	7	
Observed values	1	102	7	0	0	0	4	2	115
	2	8	148	0	0	0	4	3	163
	3	0	0	0	0	0	0	0	0
	4	0	0	0	0	0	0	0	0
	5	1	0	0	0	0	0	0	1
	6	3	2	0	0	0	21	0	26
	7	1	0	0	0	0	0	10	11
	Total	115	157	0	0	0	29	15	281
				TP+TN					281
				TP+FP+FN+TN					316
				Accuracy					89%

TP= true positive; TN= true negative; FP= false positive; FN= false negative.

For the RF algorithm, the confusion of class 1 was minimal with class 2, 6, and 7; an accuracy of 89% was obtained with this algorithm (Table 5).

Table 5. Confusion matrix for the RF algorithm.

RF		Predicted values							Total
		1	2	3	4	5	6	7	
Observed values	1	104	10	0	0	0	6	3	123
	2	7	147	0	0	0	2	0	156
	3	0	0	0	0	0	0	0	0
	4	0	0	0	0	0	0	0	0
	5	1	0	0	0	0	0	0	1
	6	2	0	0	0	0	21	2	25
	7	1	0	0	0	0	0	10	11
	Total	115	157	0	0	0	29	15	282
				TP+TN					282
				TP+FP+FN+TN					316
				Accuracy					

TP= true positive; TN= true negative; FP= false positive; FN= false negative.

DOI: https://doi.org/10.29312/remexca.v16i1.3369

The minimum distance algorithm yielded an accuracy of 48%, whereas an accuracy of 43% was obtained for the ML algorithm, and an accuracy of 46% for the SAM algorithm. These three algorithms presented the lowest accuracy values.

According to the matrices and accuracy values, when comparing the algorithms executed in GEE *versus* in QGIS, it was found that the highest percentages were obtained with the algorithms executed in GEE, which reached 89% accuracy, except for SVM, which had 59%; in contrast, those estimated with the QGIS algorithms were lower and ranged between 40 and 50%. This corroborates that the best estimated results were from the GEE platform, at least, that could be calculated with the 43 samples that were used to validate the classifications.

There is no previous study of the region that estimates agricultural areas; however, the official source of information (SIAP, 2021) provides monthly data on the progress of plantings by crop, which is comparable to the results obtained in this work (Table 1). When collating the information, it was observed that the areas are skyrocketing; for example in chili, where SIAP (2021) reported up to four times more than estimated in this work. Knowing that this methodology is based on a mathematical model, it is known that the estimated final result will have a percentage of error compared to the actual data.

On the other hand, during the methodological process, an error was detected in the execution of the field sampling, which was not covered in its entirety according to its planning; the transcendental reason was that the sampling was carried out in a short period of time and it is not that the sampling could not be prolonged for more days, but when the plots were visited, some of them were already harvested with remains of the crop or the producers were harvesting their crops and, in the best of cases, the crop was still standing.

In addition to this, the distribution of the samples was arranged so that a distance up to 40 km to reach the sampling area was considered because the field personnel stayed overnight in the locality of Salinas de Hidalgo. For example, those plots sampled in the locality of La Herradura, Santo Domingo, at a distance of 45 km from Salinas. An important aspect for the safety of the personnel is to guarantee their integrity in the zone and this disturbed the work schedules, which is why the personnel returned from the plots with time, calculating not to arrive at night to the place of stay.

Conclusions

The algorithms that yielded the highest accuracy were CART and RF, which are based on processing on the GEE platform, which allow for hardware, software, and time savings. This is reflected in the pre-processing, training, and execution stages of supervised classification.

Nevertheless, there is no way to replace the field sampling stage and everything that its development implies since it is an essential requirement as an input for classification. The GEE platform has come to revolutionize the way of working with remote sensing data since it strengthens the help of users in saving human, computer, and economic resources by being an open access platform.

As improvements to the methodology used in this work, we identified two that are related by the time variable; the first improvement could be to plan field sampling more in advance to meet 100% in form and time. The other improvement is the monitoring of the climatic conditions of the place in the agricultural cycle of study to fully identify the beginning of the sowing and the subsequent conclusion of the cycle; this will help to identify the best time to carry out the field sampling.

DOI: https://doi.org/10.29312/remexca.v16i1.3369

Acknowledgements

To the National Institute of Statistics and Geography for the time and support provided to carry out the field sampling, and for the computer infrastructure for running the classifications. To the College of Postgraduates, San Luis Potosí Campus, for the support and advice during the development of this work.

Bibliography

1 Abatzoglou, J. T.; Dobrowski, S. Z.; Parks, S. A. and Hegewisch, K. C. 2018. Terraclimate, a high-resolution global dataset of monthly climate and climatic water balance from 1958-2015, Scientific Data. 5(1):1-12. Doi:10.1038/sdata.2017.191.

2 Aghababaei, M.; Ebrahimi, A.; Naghipour, A.; Asadi, E.; and Verrelst, J. 2021. Vegetation types mapping using multi-temporal Landsat images in the google earth engine platform. Remote Sensing. 13(22):4683-15. https://doi.org/10.3390/rs13224683.

3 Aguilar, L. J. 2016. Big data, análisis de grandes volúmenes de datos en organizaciones. Primera edición. Alfaomega Grupo Editor. México, DF.

4 Amani, M.; Kakooei, M.; Moghimi, A.; Ghorbanian, A.; Ranjgar, B.; Mahdavi, S.; Davidson, A.; Fisette, T.; Rollin, P.; Brisco, B. and Mohammadzadeh, A. 2020. Application of google earth engine cloud computing platform, sentinel imagery and neural networks for crop mapping in Canada. Remote Sens. 12(21):3561-18. https://doi.org/10.3390/rs12213561.

5 Bravo, L. A. G.; González, G. H. y Rumayor, R. A. 2006. Sequía: vulnerabilidad, impacto y tecnología para afrontarla en el Norte-Centro de México. Instituto Nacional de Investigaciones Forestales, Agrícolas y Pecuarias (INIFAP)-CIRNOC-Campo Experimental Zacatecas. 2ª Edición. Libro técnico núm. 4. 297 p.

6 CONAGUA. 2020. Comisión Nacional del Agua. Estaciones meteorológicas automáticas (EMAS). https://smn.conagua.gob.mx/es/observando-el-tiempo/estaciones-meteorologicas-automaticas-emas.

7 Gallardo-Cruz, A; Fernández-Montes, O. A. y Rives, C. 2019. Detección de amenazas y oportunidades para la conservación en la cuenca baja del Usumacinta a partir de técnicas de percepción remota. Ecosistemas. 28(2):82-99. https://doi.org/10.7818/ECOS.1611.

8 German, L. A.; Vitale, J. P.; Waldman, C. P. y Castañeda N. 2019. Estimación de superficie de invernáculos en el partido de la plata, mediante dos algoritmos de inteligencia artificial en la plataforma Google Earth Engine. *In*: XI Congreso de AgroInformática (CAI) JAIIO. 48:1-11 http://sedici.unlp.edu.ar/handle/10915/88069.

9 INEGI. 2008. Instituto Nacional de Estadística y Geografía. Unidades climáticas. https://www.inegi.org.mx/temas/climatologia/.

10 INEGI. 2020a. Instituto Nacional de Estadística y Geografía. Marco geoestadístico nacional (MGN) https://www.inegi.org.mx/temas/mg/#Descargas.

11 INEGI. 2020b. Instituto Nacional de Estadística y Geografía. Geomediana Landsat https://www.inegi.org.mx/investigacion/geomediana/.

12 Killough, B. 2018. Overview of the open data cube initiative. *In*: IGARSS 2018-2018 IEEE international geoscience and remote sensing symposium. 8629-8632 pp.

13 Kok, Z. H.; Shariff, A. R. M.; Alfatni, M. S. M. and Kairunniza-Bejo, S. 2021. Support vector machine in precision agriculture: a review. Comput. Electron. Agric. 191:106546-12. https://doi.org/10.1016/j.compag.2021.106546.

14 Mananze, S.; Pôças, I. and Cunha, M. 2020. Mapping and assessing the dynamics of shifting agricultural landscapes using google earth engine cloud computing, a case study in Mozambique. Remote Sensing. 12(8):1279-23. https://doi.org/10.3390/rs12081279.

DOI: https://doi.org/10.29312/remexca.v16i1.3369

15 Núñez-López, D.; Muñoz-Robles, V. M.; Reyes-Gómez. I.; Velasco-Velasco, I. y Gadsden-Esperza, H. 2007. Caracterización de la sequía a diversas escalas de tiempo en México. Agrociencia. 41(3):253-262.

16 Panagiotakis, C.; Papadakis, H. and Fragopoulou, P. 2021. A dual hybrid recommender system based on SCoR and the random forest. Computer Science and Information Systems. 18(1):115-128. https://doi.org/10.2298/CSIS200515046P.

17 Perilla, G. A. y Mas, J. F. 2020. Google Earth Engine (GEE): una poderosa herramienta que vincula el potencial de los datos masivos y la eficacia del procesamiento en la nube. Investigaciones Geográficas. 101:1-6. https://doi.org/10.14350/rig.59929.

18 Roberts, D.; Mueller, N. and Mcintyre, A. 2017. High-dimensional pixel composites from earth observation time series. IEEE Transactions on Geoscience and Remote Sensing. 55(11):6254-6264. Doi: 10.1109/TGRS.2017.2723896.

19 Romero, F. S. 2006. La teledetección satelital y los sistemas de protección ambiental. Quivera Revista de Estudios Territoriales. 8(1):315-356.

20 Sánchez-Pozo, N.; Trilles-Oliver, S.; Solé-Ribalta, A.; Lorente-Leyva, L.; Mayorca-Torres, D. and Peluffo-Ordóñez D. 2021. Algorithms air quality estimation: a comparative study of stochastic and heuristic predictive models, lecture notes in computer science. 12886:293-304. https://doi.org/10.1007/978-3-030-86271-8-25.

21 SIAP. 2020. Servicio de Información Agroalimentaria y Pesquera. Frontera agrícola serie II. http://infosiap.siap.gob.mx/gobmx/datosAbiertos.php.

22 SIAP. 2021. Servicio de Información Agroalimentaria y Pesquera. Avance de siembras y cosechas. https://nube.siap.gob.mx/cierreagricola/.

23 Strzelecka, A. and Zawadzka, D. 2021. Application of classification and regression tree (CRT) analysis to identify the agricultural households at risk of financial exclusion. Procedia Computer Science. 192:4532-4541. https://doi.org/10.1016/j.procs.2021.09.231.

24 TA, V. G.; Douriet-Angulo, A.; Tirado-Ramírez, M. A.; López-Urquídez, G. A. and López-Orona, C. A. 2022. Root rot and wilt caused by *Fusarium* Nygamai of bean (*Phaseolus vulgaris*) in Sinaloa, México. Plant Disease. 106(10):2748-2. https://doi.org/10.1094/pdis-01-22-0123-pdn.

25 Vega, P. J. J.; Zárate-Gómez, R.; Minaya, V. R. J.; Brañas, M. M. y Benavides, R. J. E. 2019. Predicción de la pérdida de la cobertura vegetal por aumento de áreas urbanas en Iquitos, Perú. Ciencia Amazónica. 7(1):37-50. https://doi.org/10.22386/ca.v7i1.263.

26 Venkatappa, M.; Sasaki, N.; Shrestha, R. P.; Tripathi, N. K. and Ma, H. O. 2019. Determination of vegetation thresholds for assessing land use and land use changes in Cambodia using the google earth engine cloud-computing platform. Remote Sensing. 11(13):1514-30. https://doi.org/10.3390/rs11131514.

Revista Mexicana de Ciencias Agrícolas

DOI: https://doi.org/10.29312/remexca.v16i1.3369

Estimation of agricultural areas through cloud processing for the Potosino highlands

Journal Information
Journal ID (publisher-id): remexca
Title: Revista mexicana de ciencias agrícolas
Abbreviated Title: Rev. Mex. Cienc. Agríc
ISSN (print): 2007-0934
Publisher: Instituto Nacional de Investigaciones Forestales, Agrícolas y Pecuarias

Article/Issue Information
Date received: 01 October 2024
Date accepted: 01 February 2025
Publication date: 12 March 2025
Publication date: Jan-Feb 2025
Volume: 16
Issue: 1
Electronic Location Identifier: e3369
DOI: 10.29312/remexca.v16i1.3369

Categories

Subject: Articles

Keywords:

Keywords:

crops

google earth engine

QGIS

Counts

Figures: 3

Tables: 5

Equations: 0

References: 26

Pages: 0